Received 13 June 2024; accepted 2 July 2024. Date of publication 5 July 2024; date of current version 24 July 2024.
The review of this article was arranged by Editor K. Nomura.

Digital Object Identifier 10.1109/JEDS.2024.3424545

Study of Highly Stable Nitrogen-Doped a-InGaSnO Thin-Film Transistors

WENYANG ZHANG [1], LI LU [1], CHENFEI LI [1], WEIJIE JIANG [1], WENZHAO WANG [1], XINGQIANG LIU [2], ABLAT ABLIZ [3], AND DA WAN [1]

1 School of Information Science and Engineering, Wuhan University of Science and Technology, Wuhan 430081, China
2 State Key Laboratory for Chemo/Biosensing and Chemometrics, College of Semiconductors (College of Integrated Circuits), Hunan University, Changsha 410082, China
3 School of Physics and Technology, Xinjiang University, Ürümqi 830046, China

CORRESPONDING AUTHORS: D. WAN AND A. ABLIZ (e-mail: wanda@wust.edu.cn; ablatabliz@xju.edu.cn)

This work was supported in part by the National Natural Science Foundation of China under Grant U22A2074, Grant 61904129, and Grant 62064012; in part by the National Key Research and Development Program of Ministry of Science and Technology under Grant 2022YFA1402504; in part by the China National Funds for Distinguished Young Scientists under Grant 61925403; and in part by the Tianshan Talent Innovation and Technology Cultivation Project Foundation of Xinjiang Uygur Autonomous Region under Grant 2022TSYCCX0018.

ABSTRACT Herein, highly stable nitrogen (N) doped amorphous indium gallium tin oxide (a-IGTO) thin-film transistors (TFTs) are prepared and the effects of N-doping are investigated. Compared with undoped a-IGTO TFTs, a-IGTO TFTs with 6 min N plasma treatment exhibit superior bias stress stability and a threshold voltages (V_{th}) closer to 0 V with almost no decline in mobility. In particular, the positive/negative bias stress threshold shift of N-doped a-IGTO TFTs is substantially reduced in both dark and light environment. The X-ray photoelectron spectroscopy analysis (XPS) and low frequency noise (LFN) are employed to study the mechanism of N-doping in a-IGTO TFTs. The XPS results indicate that appropriate amount of N-doping could enhance the bias stress stability and control the V_{th} efficiently by passivating the defects such as oxygen vacancy in a-IGTO films. The LFN results illustrate that the average interfacial trap density could be reduced by N-doping. Overall, the strategy presented here is effective for preparing a-IGTO TFTs with enhanced stability for potential applications in future optoelectronic displays.

INDEX TERMS Amorphous indium gallium tin oxide (a-IGTO), thin-film transistors (TFTs), N doping, bias stress stability, low frequency noise (LFN).

I. INTRODUCTION

Zinc oxide (ZnO) based amorphous oxide semiconductor (AOS) thin film transistors (TFTs), such as amorphous indium zinc oxide (a-IZO) and indium gallium zinc oxide (a-IGZO) TFT, have been widely used in flat panel displays because of their excellent electrical performance and low manufacturing cost during past decade [1], [2], [3]. However, the inferior bias stress stability and low field effect mobility (usually 1∼10 cm^2/V·s) of these ZnO-based TFTs usually limit their practical applications for ultra-high resolution and large area displays [4]. Recently, amorphous indium gallium tin oxide (a-IGTO) as one of the most powerful alternative and complementary materials to a-IGZO has attracted more and more attention [5], [6], [7]. By contrast, a-IGTO TFT has a higher mobility, which is due to the s orbital overlap of In and Sn is greater than the overlap of In and Zn, and this finally enhances the permeation conduction path [8], [9], [10]. In addition, the oxygen bonding energy of Sn (528 kJ/mol) is stronger than that of Zn (250 kJ/mol), which could further improve device stability.

As reported in the literatures, a-IGTO TFTs have been well prepared using various fabrication methods, such as atomic layer deposition, solution process, and magnetron sputtering [6], [7], [11]. All these devices demonstrate excellent electrical performance with a relatively low preparation temperature. However, the bias stress stability of a-IGTO TFTs still needs to be further enhanced, especially the stability in a light environment. Meanwhile, the significant deviation of the threshold voltages (V_{th}) from 0 V is also a problem for a-IGTO TFTs in low power consumption applications. Hence, a method that can control the V_{th} shift and enhance bias stress stability without damaging mobility needs to be proposed. Plasma treatment has been demonstrated as an efficient strategy to modulate the carrier concentration and reduce the defect states associated with oxygen vacancies (V_O) in ZnO-based AOS TFTs [12]. Oxygen (O) plasma has been proved to be effective for reducing V_O in a-IGTO TFTs [13]. However, it will significantly reduce the V_O concentration and increase the surface roughness of the film, resulting in a sharp decline in performance [14]. Nitrogen (N) has been confirmed to serve as both an acceptor and a defect binder in a-IGZO TFTs to improve the bias stress stability of a-IGZO TFTs [15], [16]. Compared with O plasma, N plasma is considered more friendly to improve the thin-film properties [14]. In view of this, N plasma treatment is an ideal strategy to address the issues of a-IGTO TFTs.

Herein, we studied the a-IGTO TFTs with different N-doping levels via a magnetron sputtering and N plasma treatment. With appropriate N-doping, the reliability of a-IGTO TFTs are greatly improved both in dark and light environment. Simultaneously, the V_{th} shifted to 0 V alone with a relative undamaged field-effect mobility (μ_{FE}). To understand the charge trap mechanisms of N in a-IGTO TFTs, X-ray photoelectron spectroscopy (XPS) and low-frequency noise (LFN) analyses are carried out. The XPS results indicate that N plasma treatment could suppresses the formation of excess V_O effectively. The LFN result demonstrates that N plasma treatment could reduce the interface trap density in a-IGTO TFTs. All these results show that N-doping could enhance the stability and control the V_{th} of a-IGTO TFTs by passivating the defects and improving interface quality.

II. DEVICE STRUCTURE AND EXPERIMENTAL

The schematic view of the N-doped a-IGTO TFTs fabricated and characterized in this study is depicted in Fig. 1(a). First, 20 nm a-IGTO thin film is deposited using radio frequency (RF) magnetron sputtering on a 100 nm SiO_2 coated p^+-Si substrate with a IGTO ceramic target (In_2O_3:Ga_2O_3:SnO_2 = 7:2:1 mol%). During the deposition process, the RF power was set as 40 W, the substrate pressure was below 3×10^{-4} Pa, the Ar gas flow rate was 15 sccm, the sputtering chamber pressure was maintained at 0.8 Pa, and the substrate temperature was fixed at 100 °C. After the deposition, the a-IGTO thin film is directly treated in the aforementioned RF magnetron sputtering system using N_2 plasma with a gas mixing ratio of N_2:Ar = 20:40. The plasma treatment times are 0, 3, 6, 9, and 12 min, respectively. Finally, 100 nm Al source/drain electrodes are prepared using a direct current sputtering process. The a-IGTO thin film and Al electrodes are patterned with matching metal shadow masks, and the channel length (L) and width (W) are designed to be 120 μm and 150 μm, respectively.

III. CHARACTERIZATION AND DISCUSSION

All the electrical performance characterizations of the N-doped a-IGTO TFTs are performed under ambient conditions. An Agilent B2912 analyzer with a Lakeshore probe station is used for the electrical measurements, and an

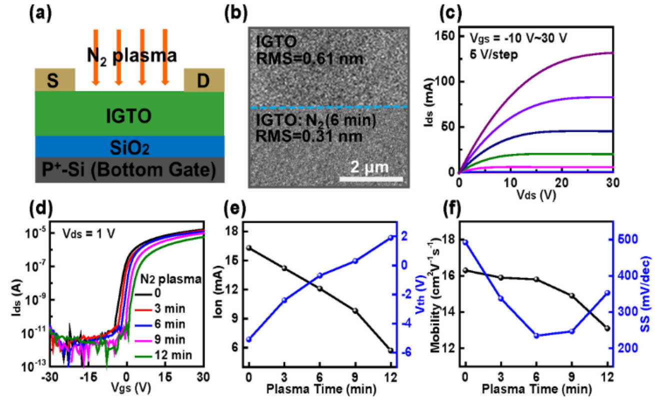

FIGURE 1. (a) Schematic view of the N-doped a-IGTO TFTs. (b) AFM images of a-IGTO TFTs with 0 and 6 min N plasma treatment. (c) Typical output characteristics of a-IGTO TFTs with 6 min N plasma treatment. (d) Typical transfer characteristics (with I_{ds} plotted logarithmically) of N-doped a-IGTO TFTs with different N plasma treatment time at V_{ds} = 1 V. (e) and (f) I_{on}, V_{th}, μ_{FE}, and SS of N-doped a-IGTO TFTs with different N plasma treatment time.

NC300L LFN analyzer is employed for the LFN measurements.

To evaluate the effect of N plasma treatment to the film surface roughness, the surface topographies of the a-IGTO thin films with different plasma treatment times were measured by an atomic force microscope (AFM). The AFM images for 0 and 6 min are shown in Fig. 1(b). The results show that the N plasma treatment has an effect on the surface roughness of the a-IGTO films. The root means square roughness (RMS) of undoped a-IGTO films is 0.61 nm, and the RMS is reduced to 0.31 nm after N-doping. A rough interface usually appears as deep valleys that act as carrier traps and scattering centers [17]. A smaller RMS result indicates that N plasma treatment could weaken the surface scattering effect and is benefits to the carrier mobility and contact resistance between the source-drain electrode and the a-IGTO thin film. Unfortunately, an excessive treatment time will introduce physical damage and interface defects to the film surface and increase the surface roughness [12].

Fig. 1(c) exhibits the output characteristic of a-IGTO TFT with 6 min N plasma treatment. The gate-source voltage (V_{gs}) changes from −10 to 30 V with a 5 V step. The saturation and conspicuous pinch-off characteristics indicate that the channel layer can be significantly modulated by the gate potential. Besides, the gate-drain current (I_{ds}) increases linearly in the small gate drain voltage (V_{ds}) region illustrates that the channel layer and the source/drain are ohmic contact [18]. The transfer characteristic curves of a-IGTO TFTs with N plasma treatment times of 0, 3, 6, 9, and 12 min at V_{ds} is 1 V and the V_{gs} is swept from −30 to 30 V is displayed in Fig. 1(d). All the transfer curves show a typical n-type characteristics with an on/off ratio of 10^7. To better characterize the effect of N-doping in a-IGTO TFTs, the key electrical performance parameters of the device are extracted. Fig. 1(e) shows the N-doping effect on ON-state channel current (I_{on}) and V_{th} of the N-doped a-IGTO TFTs. The V_{th}, which is extracted by the horizontal intercept of the linear region of the $I_{ds}^{1/2}$ versus V_{ds} plot, shifts to the right from −5.1 to 1.9 V as the N plasma treatment time increases from 0 to 12 min. Meanwhile, the I_{on} decreases as N plasma treatment time increases. These results demonstrate that N-doping is a p-type doping for a-IGTO TFTs. The positive shift of V_{th} and the reduction of I_{on} are interpreted to be associated with the decrease of electron concentration (n_e) [19]. The n_e can be calculated using the following equation [20], [21]:

$$n_e = \frac{I_{on}L}{qSV_{ds}\mu_{FE}}$$

where S is the cross-sectional area of the active layer. The n_e value of N plasma treatment time increased from 0 to 12 min are decreased from 2.5×10^{18} to 0.9×10^{18} cm^{-3}, respectively. In general, the V_O supply the electrons [12]. Thus, the decrease of n_e also proved that N doping inhibits the generation of V_O in a-IGTO TFTs.

The μ_{FE} and subthreshold swing (SS) as a function of N-doping is plotted in Fig. 1(f). The value of μ_{FE} can be calculated by the following equation [22]:

$$\mu_{FE} = \frac{g_m L}{WC_i V_{ds}}$$

where C_i is the capacitance per unit area of SiO_2, g_m is the transconductance and is obtained by the equation of $g_m = dI_{ds}/dV_{gs}$. The resulting μ_{FE} for 0, 3, 6, 9, and 12 min N plasma treatment time are 16.3, 15.9, 15.8, 14.9, and 13.1 $cm^2/V\cdot s$, correspondingly. It is delightful that although n_e is obviously decreased as the N plasma time increase, the μ_{FE} is slightly decreased. That is mainly because the N-doping could inhibit the generation of V_O as discussed in the n_e, and the V_O usually act as electron traps in the TFTs [23], [24].

To verify the N plasma treatment could reduce charge traps, SS of these TFTs are also extracted from the formula: $SS = dV_{gs}/d\log I_{ds}$. In general, the SS value is related to the interface trap density (D_{it}) between the a-IGTO channel layer and the SiO_2. The D_{it} could be estimated based on the following equation [25]:

$$D_{it} = \left(\frac{qSS}{k_B T\ln 10} - 1\right)\frac{C_i}{q}$$

where T is the temperature during measurements and k_B is Boltzmann's constant. It could be seen that the a-IGTO TFT with 6 min N plasma treatment has a minimum SS compared with other TFTs, with the resulting D_{it} of 0.76×10^{12} $cm^{-2}eV^{-1}$, which is superior to that of the undoped a-IGTO TFT with a value of 1.33×10^{12} $cm^{-2}eV^{-1}$. These results demonstrate that the N-doping can also reduce D_{it} and improve the interface quality between the a-IGTO and SiO_2.

The charge trapping in the gate dielectric and/or at the channel/dielectric interface would cause a V_{th} shift (ΔV_{th}) under positive/negative bias voltage stress [26]. To demonstrate the inhibition of defects by N-doping, the bias

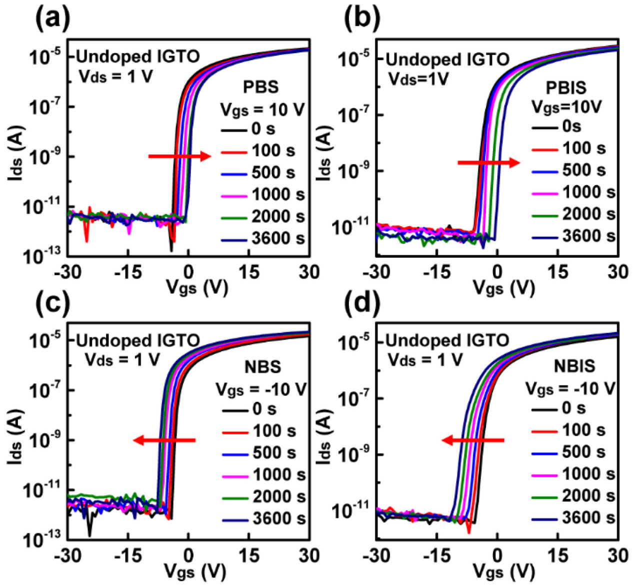

FIGURE 2. **(a)-(d) The PBS, PBIS, NBS, and NBIS of undoped a-IGTO TFTs at Vgs = ±10 V and stress duration of 3600 s.**

stress stabilities of a-IGTO TFTs with 0 and 6 min N plasma treatment at V_{gs} = 10 V and −10 V, under dark and light environments, and stress duration of 3600 s are investigated.

Fig. 2(a)-(d) presents the positive gate-bias stress (PBS), light illumination positive gate-bias stress (PBIS), negative gate-bias stress (NBS), and light illumination negative gate-bias stress (NBIS) of undoped a-IGTO TFT, respectively. The undoped a-IGTO TFT shows ΔV_{th} of 3.63 V for PBS and −3.44 V for NBS, as shown in Fig. 2(a)and(c). When introducing the illumination condition, the gate-bias stress stability becomes worse and the ΔV_{th} becomes 4.77 V for PBIS and −4.45 V for NBIS, as plotted in Fig. 2(b)-(d). The increase in ΔV_{th} mainly comes from the photo-desorption of oxygen-related species under light illumination [27]. Meanwhile, the gate-bias stress of a-IGTO TFTs with 6 min N plasma treatment is depicted in Fig. 3(a)-(d). Both under dark and light condition, the N-doped a-IGTO TFT exhibits a small ΔV_{th} for PBS (0.59 V), NBS (−0.62 V), PBIS (0.81 V), and NBIS (−0.9 V) compared with the undoped a-IGTO TFT.

The ΔV_{th} under gate-bias stress could be attributed to temporal charge trapping in the channel region and/or at the interface and the charge trap state results from the V_O has been confirmed [28]. The detailed plots of V_{th} shift versus stress time of a-IGTO TFTs with 0 and 6 min N plasma treatment are depicted in Fig. 4(a)-(b) and a significant decrease of ΔV_{th} can be seen in N-doped a-IGTO TFT. This result indicates that the N-doping could enhance bias stress stability of the a-IGTO TFT. In other words, with appropriate N-doping, the generation of V_O could be effectively suppressed, and finally cause a small ΔV_{th} and enhancement in bias stress stability for a-IGTO TFT. This conclusion is consist with the previous results and

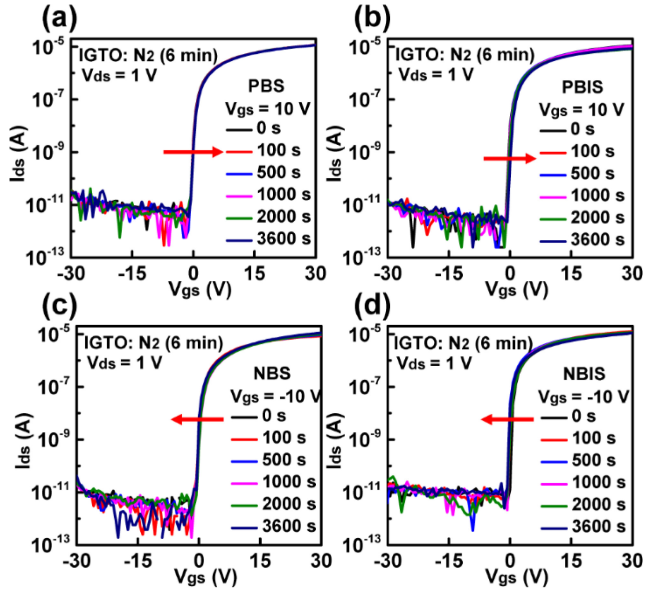

FIGURE 3. (a)-(d) The PBS, PBIS, NBS, and NBIS of a-IGTO TFTs with 6 min N plasma treatment at Vgs = ±10 V and stress duration of 3600 s.

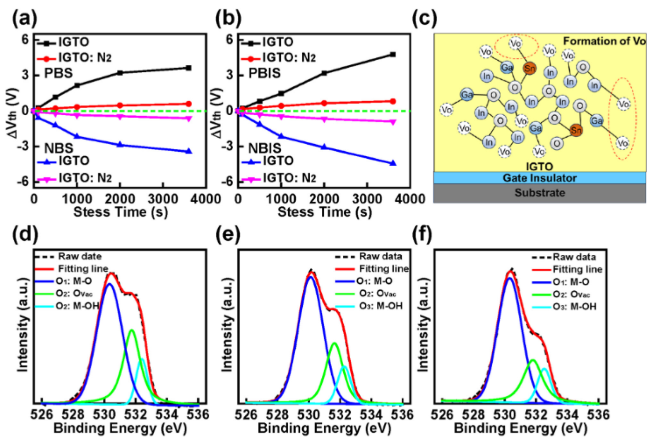

FIGURE 4. (a) The detailed plot of ΔV_{th} versus stress time of the a-IGZO with 0 and 6 min N plasma treatment under PBS and NBS. (b) The detailed plot of ΔV_{th} versus stress time of the a-IGZO with 0 and 6 min N plasma treatment under PBIS and NBIS. (c) Schematic view of interfaces trap sites and V_O defect states in the a-IGTO TFT. (d)-(f) O 1s XPS spectra of the a-IGTO thin film with 0, 6, and 12 min N plasma treatment.

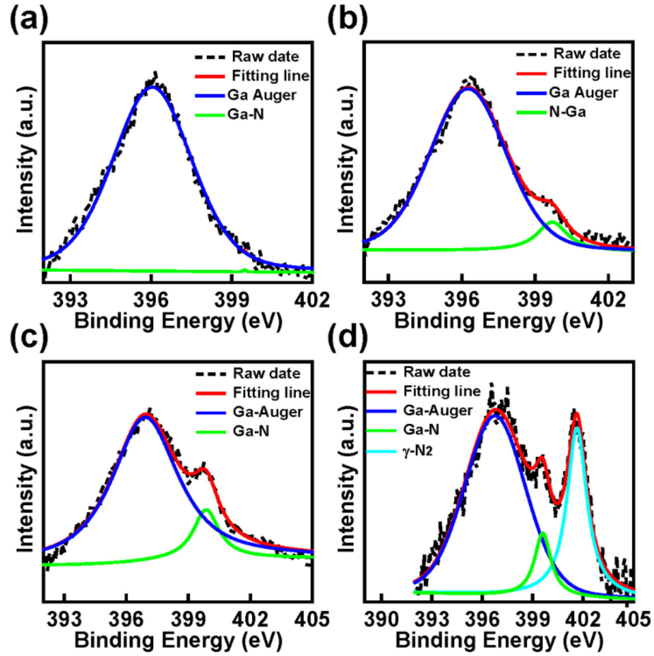

FIGURE 5. (a)-(d) N 1s XPS spectra of the a-IGTO thin film with 0, 6, 9, and 12 min N plasma treatment.

discussions about the n_e and D_{it}. The N-doped a-IGTO TFT obtains a better gate-bias stress stability while compared with undoped a-IGZO TFT and the relevant reason is that the traps associated with V_O are constantly suppressed by the N-doping.

Fig. 4(c) depicts the interfaces trap sites and V_O defect states of the a-IGTO thin films. The doping principle lies that the N would replace these V_O and form N-metal bond by attaching to metal ions after N plasma treatment [12], [14], [29]. To verify the detailed principle of N-doping, the O 1s and N 1s bonding properties of N-doped a-IGTO thin films are analyzed by XPS.. The O 1s spectra of a-IGTO TFT with 0, 6, and 12 min N plasma treatment are carefully deconvoluted into three different peaks, centered at 529.9 ± 0.1, 530.7 ± 0.1, and 531.9 ± 0.1 eV, respectively, as shown in Fig. 4(d)-(f) [30]. The area of $O_2 = (O_2/O_1+O_2+O_3)$ decreases from 32.6% to 26.7% to 21.4% as the N plasma treatment time increases from 0 to 6 to 12 min, indicating that the V_O are reduced by the N plasma treatment. This result illustrates the N-doping could significantly reduce V_O defect states in the active channel layer of the a-IGTO thin films and improve the bias stress stability, which is consists with the above discussion. The experimental curve of the N 1s XPS spectra of a-IGTO thin films with 0, 6, 9, and 12 min N plasma treatment are exhibited in Fig. 5(a)-(d). As the N plasma time is increased to 6 and 9 min, the peak shift to higher energy. Besides, the N-Ga peak start to appear and gradually increased [16]. When the N plasma time increased to 12 min, the peak of γ-N_2 (relating to adsorbed nitrogen molecules or impurities) is appear, suggesting that there are more defects (non-reacted N_2 molecules) introduced into a-IGTO films if too many nitrogen atoms were doped [31]. The N 1s XPS spectra indicates N is successfully doped in a-IGTO thin films.

To further verify the impacts of N plasma treatment to the trap density, the LFN measurement is carried out for the a-IGTO TFTs with 0, 6, and 12 min N plasma treatment. Fig. 6(a) shows the relationship between normalized drain-current noise spectral densities (S_{ID}/I_D^2) and frequency (f) of a-IGTO TFT with 6 min N plasma treatment. It is apparent that all the curves fit classical 1/f noise model very well when the (V_{gs}-V_{th}) ranging from 1 to 5 V and the f ranging from 1 to 1000 Hz [32]. Subsequently, the LFN measurements of a-IGTO TFTs with 0, 6, and 12 min N plasma treatment are

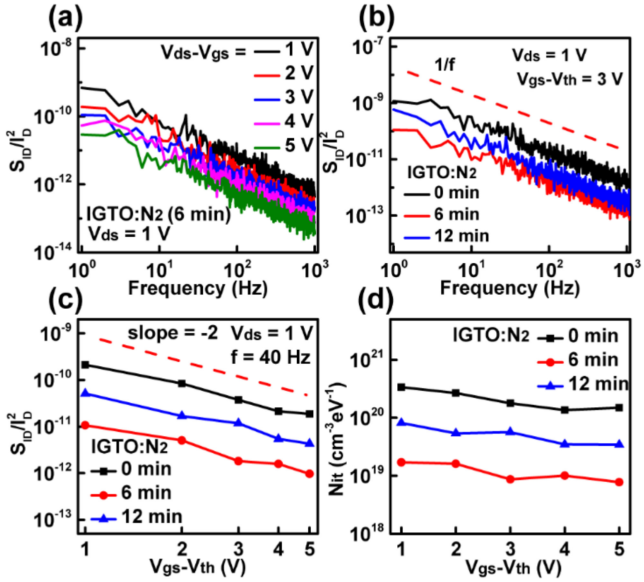

FIGURE 6. (a) Typically normalized LFN spectrum of the a-IGTO TFTs with 6 min N plasma treatment at V_{ds} = 1 V and (V_{gs}-V_{th}) ranging from 1 to 5 V. (b) Typically normalized LFN spectrum of the a-IGTO TFTs with 0, 6, and 12 min N plasma treatment at (V_{gs}-V_{th}) = 3 V and V_{ds} = 1 V. (c) Normalized S_{ID}/I_D^2 as a function of (V_{gs}-V_{th}) log-log plots of he a-IGTO TFTs with 0, 6, and 12 min N plasma treatment at f = 40 Hz and V_{ds} = 1 V. (d) The calculated N_{it} as a function of different over drive gate voltage.

conducted to make a comparison at (V_{gs}-V_{th}) = 3 V and V_{ds} = 1 V, as shown in Fig. 6(b). In general, carrier number fluctuation (ΔN) and correlated mobility fluctuation ($\Delta\mu$) are used to explain the origin of the 1/f noise [33]. The ΔN theory explains the origin of 1/f noise as the generation-recombination noise in the electron transitions between the conduction band of the channel material and the traps in the oxide layer. While the $\Delta\mu$ theory regards the fluctuations in mobility of free carriers in conducting channel as the origin of 1/f noise [33], [34]. The relationship between S_{ID}/I_D^2 and (V_{gs}-V_{th}) is fitted in Fig. 6(c) at V_{ds} = 1 V and f = 40 Hz. All three TFTs show an approximate slope value of −2, indicating the origin of 1/f noise is caused by ΔN theory [30]. According to the 1/f noise model, the average interfacial trap density (N_{it}) within the gate oxide could be estimated by the following equation [35]:

$$N_{it} = \frac{S_{ID} C_i^2 WLf\left(V_{gs} - V_{th}\right)\gamma}{q^2 k_B T I_D^2}$$

where γ is 10^8 cm^{-1} for the Si-SiO_2 system [32]. The calculated N_{It} value of a-IGTO TFTs with 0, 6, and 12 min N plasma treatment at f = 40 Hz and (V_{gs}-V_{th}) changes from 1 to 5 V is shown in Fig. 6(d). The curve reflects the approximately uniform oxide trap distribution in each device. The N_{it} are calculated to be 1.8×10^{20}, 8.7×10^{18}, and 5.66×10^{19} for 0, 6, and 12 min N plasma treated a-IGTO TFTs, respectively. This result is consistent with the above discussion about D_{it} estimated from SS. It further proves that moderate N-doping could reduce defects in the channel layer, while excessive N plasma treatment will introduce additional defects to the thin film.

IV. CONCLUSION

In summary, the a-IGTO TFTs with varied N-doping degree are obtained via a N plasma treatment approach. By rationally modulating the treating time, superior bias stress stability, V_{th} closer to 0 V, and almost no decline in mobility are simultaneously achieved in the a-IGTO TFTs with 6 min N plasma treatment. Specifically, the a-IGTO TFTs with 6 min N plasma treatment shows a V_{th} of −0.5 V, a μ_{FE} of 15.8 cm^2/V·s, a SS of 235 mV/dec, and a small ΔV_{th} for PBS (0.59 V), NBS (−0.62 V), PBIS (0.81 V), and NBIS (−0.9 V). The XPS results suggest that N plasma treatment could enhance the bias stress stability and control the V_{th} efficiently through passivating the defects such as V_O in the a-IGTO films. The LFN results indicate N-doping could decrease N_{it} and improve interface quality effectively. Therefore, the fabrication of N-doped a-IGTO TFTs has deep potential for low-power and high resolution flat-panel displays.

REFERENCES

[1] N. L. Dehuff et al., "Transparent thin-film transistors with zinc indium oxide channel layer," *J. Appl. Phys.*, vol. 97, no. 6, Mar. 2005, Art. no. 064505, doi: 10.1063/1.1862767.
[2] A.-H. Tai, C.-C. Yen, T.-L. Chen, C.-H. Chou, and C. W. Liu, "Mobility enhancement of back-channel-etch amorphous InGaZnO TFT by double layers with quantum well structures," *IEEE Trans. Electron Devices*, vol. 66, no. 10, pp. 4188–4192, Oct. 2019, doi: 10.1109/TED.2019.2932798.
[3] H. Li, M. Qu, and Q. Zhang, "Influence of tungsten doping on the performance of indium-zinc-oxide thin-film transistors," *IEEE Electron Device Lett.*, vol. 34, no. 10, pp. 1268–1270, Oct. 2013, doi: 10.1109/LED.2013.2278846.
[4] C. Wang et al., "High-mobility solution-processed amorphous indium zinc oxide/In_2O_3nanocrystal hybrid thin-film transistor," *IEEE Electron Device Lett.*, vol. 34, no. 1, pp. 72–74, Jan. 2013. doi: 10.1109/LED.2012.2226425.
[5] M. Hu, L. Xu, X. Zhang, Z. Song, and S. Luo, "In-situ Ar plasma treatment as a low thermal budget technique for high performance InGaSnO thin film transistors fabricated using magnetron sputtering," *Appl. Surf. Sci.*, vol. 604, Dec. 2022, Art. no. 154621, doi: 10.1016/j.apsusc.2022.154621.
[6] S.-H. Noh et al., "Improvement in short-channel effects of the thin-film transistors using atomic-layer deposited In–Ga–Sn–O channels with various channel compositions," *IEEE Trans. Electron Devices*, vol. 69, no. 10, pp. 5542–5548, Oct. 2022, doi: 10.1109/ted.2022.3198032.
[7] Z. Wang, H. Xu, Y. Zhang, H. C. Cho, J. K. Jeong, and C. Choi, "Low temperature (<150 °C) annealed amorphous indium-gallium-tin oxide (IGTO) thin-film for flash memory application," *Appl. Surf. Sci.*, vol. 605, Dec. 2022, Art. no. 154614, doi: 10.1016/j.apsusc.2022.154614.
[8] S.-H. Hwang, K. Yatsu, D.-H. Lee, I.-J. Park, and H.-I. Kwon, "Effects of Al_2O_3surface passivation on the radiation hardness of IGTO thin films for thin-film transistor applications," *Appl. Surf. Sci.*, vol. 578, Mar. 2022, Art. no. 152096, doi: 10.1016/j.apsusc.2021.152096.
[9] J. Su et al., "Preparation and electrical characteristics of N-doped In-Zn-Sn-O thin film transistors by radio frequency magnetron sputtering," *J. Alloy. Compd.*, vol. 750, pp. 1003–1006, Jun. 2018, doi: 10.1016/j.jallcom.2018.04.058.
[10] B. K. Kim et al., "Polycrystalline indium gallium tin oxide thin-film transistors with high mobility exceeding 100 cm^2/Vs," *IEEE Electron Device Lett.*, vol. 42, no. 3, pp. 347–350, Mar. 2021, doi: 10.1109/LED.2021.3055940.
[11] C. Oh, H. Jung, S. H. Park, and B. S. Kim, "Enhanced electrical properties of In-Ga-Sn-O thin films at low-temperature annealing," *Ceram. Int.*, vol. 48, no. 7, pp. 9817–9823, Apr. 2022, doi: 10.1016/j.ceramint.2021.12.183.

[12] A. Abliz, P. Nurmamat, and D. Wan, "Rational design of oxide heterostructure InGaZnO/TiO2 for high-performance thin-film transistors," *Appl. Surf. Sci.*, vol. 609, Jan. 2023, Art. no. 155257, doi: 10.1016/j.apsusc.2022.155257.

[13] Z. Han, J. Han, and A. Abliz, "Enhanced electrical performance of InGaSnO thin-film transistors by designing a dual-active-layer structure," *Appl. Surf. Sci.*, vol. 648, Mar. 2024, Art. no. 158995, doi: 10.1016/j.apsusc.2023.158995.

[14] H. Xie, J. Xu, G. Liu, L. Zhang, and C. Dong, "Development and analysis of nitrogen-doped amorphous InGaZnO thin film transistors," *Mat. Sci. Semicon. Process.*, vol. 64, pp. 1–5, Jun. 2017, doi: 10.1016/j.mssp.2017.03.003.

[15] T.-H. Huang et al., "Eliminating surface effects via employing nitrogen doping to significantly improve the stability and reliability of ZnO resistive memory," *J. Mater. Chem. C*, vol. 1, no. 45, pp. 7593–7597, 2013, doi: 10.1039/C3TC31542H.

[16] X. Huang et al., "Enhanced bias stress stability of a-InGaZnO thin film transistors by inserting an ultra-thin interfacial InGaZnO: N layer," *Appl. Phys. Lett.*, vol. 102, no. 19, May 2013, doi: 10.1063/1.4805354.

[17] X. Ding, J. Yang, C. Qin, X. Yang, T. Ding, and J. Zhang, "Nitrogen-doped ZnO film fabricated via rapid low-temperature atomic layer deposition for high-performance ZnON transistors," *IEEE Trans. Electron Devices*, vol. 65, no. 8, pp. 3283–3290, Aug. 2018, doi: /10.1109/TED.2018.2848275.

[18] Z. Yang et al., "Performance limits of the self-aligned nanowire top gated MoS_2 transistors," *Adv. Funct. Mater.*, vol. 27, no. 19, May 2017, Art. no. 1602250, doi: 10.1002/adfm.201602250.

[19] D. Wan et al., "Design of highly stable tungsten-doped IZO thin-film transistors with enhanced performance," *IEEE Trans. Electron Devices*, vol. 65, no. 3, pp. 1018–1022, Mar. 2018, doi: 10.1109/TED.2018.2797300.

[20] L. Xu et al., "The different roles of contact materials between oxidation interlayer and doping effect for high performance ZnO thin film transistors," *Appl. Phys. Lett.*, vol. 106, no. 5, Feb. 2015, Art. no. 051607, doi: 10.1063/1.4907680.

[21] D. Wan et al., "The study for solution-processed alkali metal-doped indium-zinc oxide thin-film transistors," *IEEE Electron Device Lett.*, vol. 37, no. 1, pp. 50–52, Jan. 2016, doi: 10.1109/LED.2015.2501290.

[22] E. Fortunato, P. Barquinha, and R. Martins, "Oxide semiconductor thin-film transistors: A review of recent advances," *Adv. Mater.*, vol. 24, no. 22, pp. 2945–2986, Jun. 2012, doi: 10.1002/adma.201103228.

[23] W.-S. Kim et al., "The influence of hafnium doping on bias stability in zinc oxide thin film transistors," *Solid Film*, vol. 519, no. 15, pp. 5161–5164, May 2011, doi: 10.1016/j.tsf.2011.01.079.

[24] K. Ide, Y. Kikuchi, K. Nomura, M. Kimura, T. Kamiya, and H. Hosono, "Effects of excess oxygen on operation characteristics of amorphous In-Ga-Zn-O thin-film transistors," *Appl. Phys. Lett.*, vol. 99, no. 9, Aug. 2011, Art. no. 093507, doi: 10.1063/1.3633100.

[25] R. M. B. Cross, M. M. D. Souza, S. C. Deane, and N. D. Young, "A comparison of the performance and stability of ZnO-TFTs with silicon dioxide and nitride as gate insulators," *IEEE Trans. Electron Devices*, vol. 55, no. 5, pp. 1109–1115, May 2008, doi: 10.1109/TED.2008.918662.

[26] K. Hoshino, D. Hong, H. Q. Chiang, and J. F. Wager, "Constant voltage-bias stress testing of a-IGZO thin-film transistors," *IEEE Trans. Electron Devices*, vol. 56, no. 7, pp. 1365–1370, Jul. 2009, doi: 10.1109/TED.2009.2021339.

[27] A. Abliz et al., "Enhanced reliability of In-Ga-ZnO thin-film transistors through design of dual passivation layers," *IEEE Trans. Electron Devices*, vol. 65, no. 7, pp. 2844–2849, Jul. 2018, doi: 10.1109/TED.2018.2836146.

[28] Y. Jeong et al., "Bias-stress-stable solution-processed oxide thin film transistors," *ACS Appl. Mater. Interfaces*, vol. 2, no. 3, pp. 611–615, Feb. 2010, doi: 10.1021/am900787k.

[29] G. Li et al., "Nitrogen-doped amorphous InZnSnO thin film transistors with a tandem structure for high-mobility and reliable operations," *IEEE Electron. Dev. Lett.*, vol. 37, no. 5, pp. 607–610, May 2016, doi: 10.1109/LED.2016.2548020.

[30] H.-C. Chiu, C.-W. Yang, C.-H. Chen, and C.-H. Wu, "Quality of the oxidation interface of AlGaN in enhancement-mode AlGaN/GaN highelectron mobility transistors," *IEEE Trans. Electron Devices*, vol. 59, no. 12, pp. 3334–3338, Dec. 2012, doi: 10.1109/TED.2012.2215872.

[31] H. Xie, Y. Zhou, Y. Zhang, and C. Dong, "Chemical bonds in nitrogen-doped amorphous InGaZnO thin film transistors," *Results Phys.*, vol. 11, pp. 1080–1086, Dec. 2018. doi: 10.1016/j.rinp.2018.11.029.

[32] D. Wan et al., "Low-frequency noise in high-mobility a-InGaZnO/InSnO nanowire composite thin-film transistors," *IEEE Electron Device Lett.*, vol. 38, no. 11, pp. 1540–1542, Nov. 2017, doi: 10.1109/LED.2017.2757144.

[33] L. K. J. Vandamme, X. Li, and D. Rigaud, "1/f noise in MOS devices, mobility or number fluctuations?" *IEEE Trans. Electron Devices*, vol. 41, no. 11, pp. 1936–1945, Nov. 1994, doi: 10.1109/16.333809.

[34] A. Abliz et al., "Effects of nitrogen and hydrogen codoping on the electrical performance and reliability of InGaZnO thin-film transistors," *ACS Appl. Mater. Interfaces*, vol. 9, no. 12, pp. 10798–10804, Mar. 2017, doi: 10.1021/acsami.6b1527S.

[35] K. K. Hung, P. K. Ko, C. Hu, and Y. C. Cheng, "A unified model for the flicker noise in metal-oxide-semiconductor field-effect transistors," *IEEE Trans. Electron Devices*, vol. 37, no. 3, pp. 654–665, Mar. 1990, doi: 10.1109/16.47770.